Optics Letters

Distributed dynamic strain measurement with a direct detection scheme by using a three-step-phase-shifted double pulse in a UWFBG array

Rui Hong,[1] Feng Wang,[1,*] Yong Yu,[1] Wei Jiang,[1] Yanqing Lu,[1] Lin Zhang,[2] Yixin Zhang,[1] and Xuping Zhang[1]

[1]Key Laboratory of Intelligent Optical Sensing and Manipulation, Ministry of Education, College of Engineering and Applied Sciences, Nanjing University, Nanjing 210023, China
[2]Aston Institute of Photonic Technologies, Aston University, Birmingham B4 7ET, UK
*wangfeng@nju.edu.cn

Received 11 January 2023; revised 7 February 2023; accepted 10 March 2023; posted 17 March 2023; published 11 April 2023

We demonstrate a stable homodyne phase demodulation method with a double pulse based on an ultra-weak fiber Bragg grating (UWFBG) array. The technique divides one of the probe pulses into three sections and introduces successive 2π/3 phase differences into each section. By using a simple direct detection scheme, it can achieve distributed and quantitative vibration measurement along the UWFBG array. Compared to the traditional homodyne demodulation technique, the proposed technique is more stable and easier to accomplish. Moreover, the reflected light from the UWFBGs can provide a signal that is modulated uniformly by the dynamic strain and multiple results for averaging, resulting in a higher signal-to-noise ratio (SNR). We experimentally demonstrate the technique's effectiveness by monitoring different vibrations. The SNR for measuring a generic 100 Hz, 0.08 rad vibration in a 3 km UWFBG array with a reflectivity of −40 to −45 dB is estimated to be ∼44.92 dB.

https://doi.org/10.1364/OL.485414

The potential of phase-sensitive optical time-domain reflectometry (Φ-OTDR) has been widely discussed because of its significant merits, such as high sensitivity [1], accurate localization [2], a broadband response [3], and quantitative measurement [4]. Various phase demodulation methods have been proposed for performing quantitative measurements in recent years [5–10]. These demodulation methods can be categorized into heterodyne demodulation and homodyne demodulation. Generally, heterodyne demodulation has a better signal-to-noise ratio (SNR) but cannot directly locate the disturbance. Thus, global demodulation is required, resulting in a large data processing burden. In contrast, homodyne demodulation can directly locate the disturbance through the interference-induced intensity change and avoid the impact of the reference light. However, most homodyne demodulation methods have strict requirements for some parameters, which may cause instability in practical applications. For example, the 3×3 coupler and 90° hybrid homodyne demodulation methods require high consistency of the DC component, AC coefficient, phase difference, and polarization state. The phase generated carrier (PGC) homodyne demodulation method requires the same modulation amplitude of the Bessel function. Moreover, homodyne demodulation has a smaller SNR than heterodyne demodulation due to the lack of reference light and the splitting of the signal. Considering the intrinsic disadvantages of the heterodyne demodulation technique, a stable and high-SNR homodyne demodulation method is more appropriate due to its fast positioning and freedom from the reference light.

In this Letter, we propose a novel Φ-OTDR scheme based on an ultra-weak fiber Bragg grating (UWFBG) array which can achieve stable and high-SNR homodyne demodulation. It produces a three-step-phase-shifted double pulse as the probe pulse and uses the reflected light from the UWFBG as the signal. The reflected light can provide a higher SNR than the Rayleigh backscattering (RBS) in a normal single-mode fiber. The phase change is demodulated quantitatively from the different three-step phases. This method abandons the coupler, the interferometer, and multiple photodetectors (PDs), and does not require a modulation carrier and phase unwrapping, thus significantly improving the stability and decreasing the scheme's complexity. Moreover, the introduction of the UWFBG can also provide multiple channels for averaging, further enhancing the SNR. Experimental results have shown that the dynamic strain on the fiber can be located directly and demodulated quantitatively with a high SNR.

In the conventional homodyne demodulation method with a 3×3 coupler, a Mach–Zehnder interferometer (MZI) and a symmetric 3×3 output port coupler is introduced in the direct detection scheme. Light from a narrow-linewidth laser (NLL) is modulated by an acousto-optic modulator (AOM) to create the probe optical pulse, with subsequent amplification through an Er-doped fiber amplifier (EDFA) followed by an optical circulator (CIR), as shown in Fig. 1. The probe optical pulse can

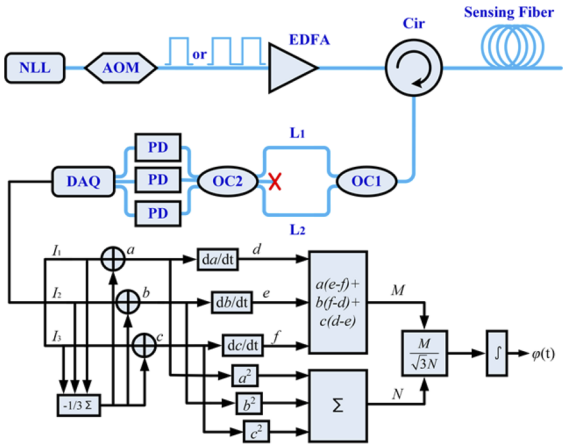

Fig. 1. Conventional setup of a Φ-OTDR system that uses the three-phase-shifted components method.

be either a single pulse [7] or a double pulse [10]. A single pulse requires different arm lengths (L1 ≠ L2) in the MZI to make two backscattering signals from different positions overlap. A double pulse needs the same lengths (L1 = L2) because the backscattering signals generated by the two optical pulses from different positions have already overlapped in the sensing fiber. Three PDs are used to receive the output optical signal of the coupler. By processing the three outputs according to a specific procedure, the phase change induced by dynamic strain can be derived.

Theoretically, the three outputs can be expressed as

$$I_k(t) = A + B\cos[\phi(t) + \phi_0 + \phi_n + (k-1)\times\frac{2\pi}{3}], k = 1, 2, 3, \quad (1)$$

where $\phi(t)$, ϕ_0, and ϕ_n are the phase change, the initial phase, and the phase noise, respectively. A denotes the DC component and B denotes the AC coefficient.

Compared with 90° hybrid demodulation, the dynamic measurement range of the 3 × 3 coupler method is not limited by the phase unwrapping because it doesn't need the arctangent operation and avoids the error induced by the near-zero denominator. Compared with PGC modulation, its frequency response is higher because there is no need for a modulation carrier. However, it is difficult to maintain perfect consistency for the DC part and the AC coefficient of the three outputs due to the imperfection of the coupler and the inconsistency of the detector's responsivity. It is difficult to keep the polarization states of the three outputs consistent unless an all-polarization-preserving system is used, which critically increases the cost, and the SNR will, in principle, be decreased due to the splitting of the signal. Moreover, the performances of the interferometer and the coupler are easily influenced by temperature changes, so thermal isolation is generally required for stable demodulation [7], which further increases the complexity of the system.

We simulated the influences of the three parameters, as shown in Fig. 2. Small deviations (1%) of the DC component, AC coefficient, and phase difference in Eq. (1) will cause harmonic distortion [Figs. 2(a)–2(c)]. As the amplitude and number of deviations increase, larger distortion occurs. Especially when all three parameters have deviations, the demodulation result will not have sufficient information [Fig. 2(d)]. Thus, it is easy for the conventional setup of a Φ-OTDR system with the three

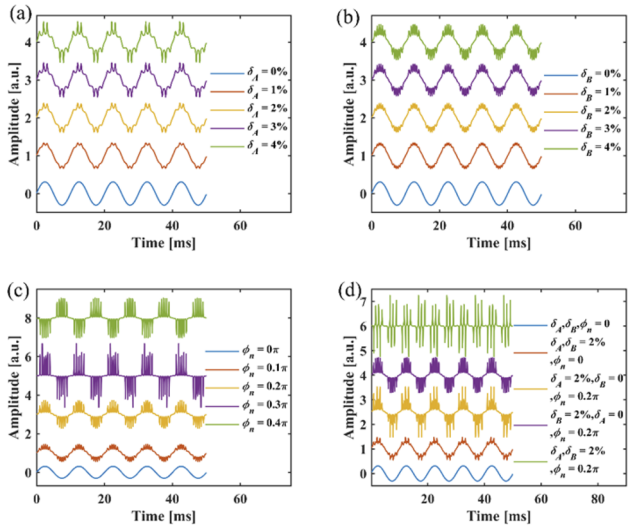

Fig. 2. Simulation results for the 3 × 3 coupler demodulation method obtained when (a) the DC component, (b) the AC coefficient, (c) the phase difference, and (d) more than one parameter deviates. Here δ_A and δ_B represent the deviation values and ϕ_n represents the phase noise.

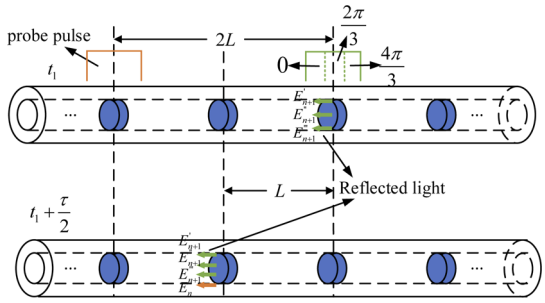

Fig. 3. Principle of using a phase-modulated double pulse in UWFBGs (L is the spacing between adjacent UWFBGs, $\tau = 2L/v$, v is the speed of light in the fiber).

phase-shifted components method to generate distortion due to poor consistency.

To solve the above-discussed problems with the three-step phase -shifting method, we introduce a novel phase-modulated double-pulse method based on a UWFBG array. The UWFBG has much higher reflectivity than the RBS, a wide reflective spectrum, and its position is fixed, therefore offering a high SNR, good stability, and excellent strain linearity [11]. The basic principle is shown in Fig. 3. We use double-pulse light as the probe light. The phase of the front pulse is modulated by a phase modulator to generate three sections with different modulated phases. The modulated phase difference is 2π/3 between adjacent sections. By setting the interval between the two pulses as twice the UWFBG interval, the reflected light of the front pulse (green) at any UWFBG can overlap with the rear pulse's reflected light (orange) at the adjacent UWFBG, forming interference. Because the three pulse regions have the same optical path in the fiber, the phase changes are nearly identical, so the 2π/3 phase difference can be maintained until the interference light is detected. Because the time interval between the three pulse regions is very tiny, the electric field amplitudes can be regarded as constant. Provided that the strain is between the nth

and $(n+1)$th UWFBGs, the reflected light generated by the three pulse regions can be represented as

$$\mathbf{E}'_{n+1}(t) = E_{n+1}\exp[j\omega t + j\phi(t)] \tag{2}$$

$$\mathbf{E}''_{n+1}(t) = E_{n+1}\exp[j\omega t + j\phi(t) + \frac{2\pi}{3}] \tag{3}$$

$$\mathbf{E}'''_{n+1}(t) = E_{n+1}\exp[j\omega t + j\phi(t) + \frac{4\pi}{3}], \tag{4}$$

where E_{n+1} is the amplitude of the electric field, ω is the angular frequency, and $\phi(t)$ is the phase change caused by the dynamic strain.

The reflected light generated by the rear pulse can be represented as

$$\mathbf{E}_n(t) = E_n\exp[j\omega t]. \tag{5}$$

When the reflected light of the front pulse overlaps with that of the rear pulse, the interference signal can also be divided into three regions and can be expressed as

$$I'(t) = {E_n}^2 + {E_{n+1}}^2 + 2E_nE_{n+1}\cos[\phi(t)] \tag{6}$$

$$I''(t) = {E_n}^2 + {E_{n+1}}^2 + 2E_nE_{n+1}\cos[\phi(t) + \frac{2\pi}{3}] \tag{7}$$

$$I'''(t) = {E_n}^2 + {E_{n+1}}^2 + 2E_nE_{n+1}\cos[\phi(t) + \frac{4\pi}{3}]. \tag{8}$$

The DC component $({E^2}_n + {E^2}_{n+1})$ and the AC coefficient $(2E_nE_{n+1})$ for the three signals are the same. Because the three light signals are transmitted in a serial way, we only need one PD to detect them, which ensures consistency and reduces complexity. Moreover, the phase modulator is more stable than the 3×3 coupler, which gives better accuracy of the phase difference. As for positioning and demodulation, the phase change caused by the disturbance will change the intensity of the light signal, as shown in Eqs. (6)–(8). Thus, we can determine whether to demodulate the phases of the light signals from their intensity fluctuations, which significantly simplifies the data processing. In addition, using Eqs. (6)–(8), quantitative measurement can be achieved.

There is another advantage of our proposed method. Since the integral and differential operations for the digital signal are approximate operations, a higher SNR is critical to achieving better results. Therefore, using the reflected light instead of the RBS and avoiding the splitting loss will achieve a better measurement result. Moreover, we can obtain many sampling points for each modulated phase from the reflected light, so we can obtain a higher SNR through the averaging operation.

The experimental setup used to demonstrate the proposed stable homodyne demodulation system is shown in Fig. 4. The output continuous-wave (CW) light of a narrow-linewidth laser source is modulated into two optical pulses by one AOM, whose frequency shift is 150 MHz. The pulse widths of the two optical pulses are both 300 ns and the period is 50 μs. The time interval between the two optical pulses is 500 ns to match the UWFBG array's spatial interval, which is 50 m between adjacent UWFBGs. A small deviation of the time interval is tolerable because most of the signal can still be effectively modulated and the pulse interval along the fiber does not change significantly. After that, the phase of the front probe pulses is modulated with a phase modulator (PM). Based on the modulation, the front optical pulse can be divided into three sections. The phase difference between every two adjacent sections is $2\pi/3$. The devices before

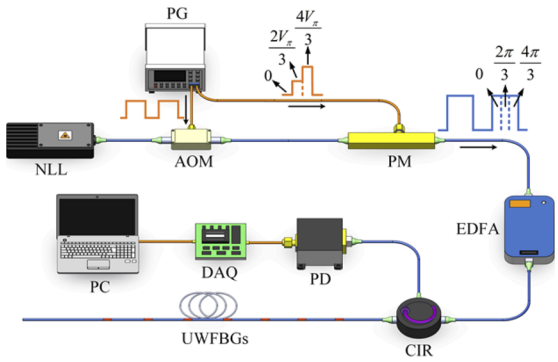

Fig. 4. Experimental setup of the proposed stable homodyne demodulation system. PG: pulse generator.

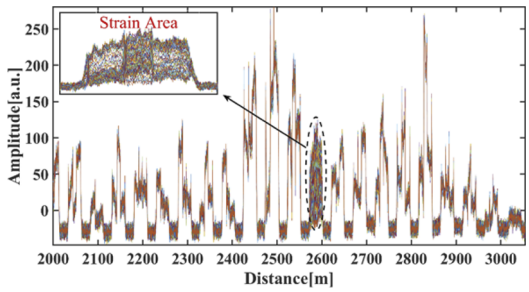

Fig. 5. Detected optical signal near the strain area (100 periods are shown together).

the PM are all polarization maintaining to ensure that the polarization state meets the crystal's fast (or slow) axis. Then, the pulse pair is amplified by an EDFA and injected into a 3 km UWFBG array via a CIR. The distance between two adjacent UWFBGs is 50 m. The returning interference signal is received by a PD. A DAQ card with a sampling rate of 500 MSa/s converts the electric signal into digital form and sends it to a computer for signal processing. It should be noted that a higher spatial resolution requires a narrower pulse width, so a phase modulator with a larger bandwidth is required. Generally, a phase modulator with a bandwidth of 1 GHz is sufficient for a spatial resolution of better than 5 m.

To test the measurement capability of our proposed phase-modulated double-pulse Φ-OTDR based on a UWFBG array, a PZT was placed at about 2.6 km. The PZT was driven by a 100 Hz sinusoidal signal. Figure 5 shows 100 time-domain curves near the vibrating area. Because the system is a homodyne scheme, the amplitude of the interference signal varies with the dynamic strain, so the dynamic strain can be easily located: it is at the 52nd UWFBG (2.6 km), as shown in Fig. 5. This feature will greatly reduce the burden of data processing, especially in long-distance sensing, compared with the heterodyne scheme, which requires global phase demodulation and the spatial derivative to locate the perturbation.

According to an enlarged figure of the dynamic strain section (the inset in Fig. 5), there are three regions with asynchronous fluctuations. From this signal, we can obtain 140 sampling points. Figure 6 shows the variations of the demodulated phases for the 140 sampling points. The phases change along time and have obvious boundaries for different fiber regions. In each region, the phase changes of different fiber positions all have

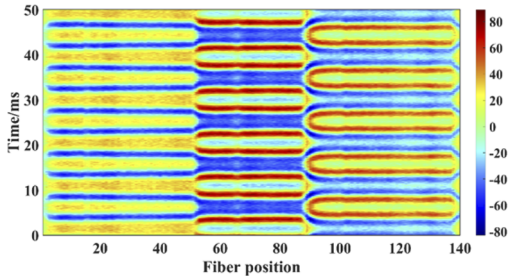

Fig. 6. Two-dimensional projection of the light intensity of the 140 sampling points on the grating.

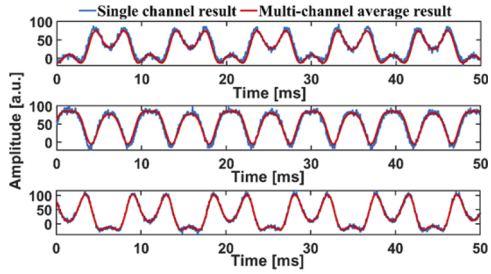

Fig. 7. Three light intensity signals with different phase modulation statuses (blue curve: single-channel result; red curve: average multi-channel result).

the same periodicity, which confirms the validity of the phase modulation of the front optical pulse.

In the procedure of signal processing, we first get three signals with different phase modulation statuses by choosing three sampling points from each region, as shown in Fig. 6. By doing the same operation for the reflection signal at different times, three signals for different times can be obtained, which are shown separately in Fig. 7 as blue curves. However, due to the influence of noise, the SNR is unsatisfactory. To get a better result, we consider using all the sampling points in the signals for demodulation. There are 140 sampling points in the three signal regions, so each region has more than 40 sampling points. Because the pulse width is 300 ns, we can ignore the phase change induced by the dynamic strain between different regions. Thus, these different sampling points can be regarded as 40 channels. Naturally, we can inhibit the noise by using the numerical average to get a better SNR, as shown in Fig. 7 by the red curve. We can see that the multi-channel average result has smaller noise fluctuations than the single-channel result.

Then, based on the signals in Fig. 7, we use the three-step phase-shifting algorithm to extract the phase information. The derived signals for the dynamic strain in the time domain and frequency domain are shown in Fig. 8. In Fig. 8(a), we can see that the waveform of the dynamic strain can be recovered accurately with an SNR of 37.18 dB. The harmonic frequency components in the simulation results (Fig. 2) are barely seen in Fig. 8, which confirms the good consistency of our method. Although the consistency of our scheme is better than that of the traditional scheme, minor inconsistencies may still exist due to the imperfection of the PM, and tiny harmonic frequency components can be seen in Fig. 8(b). After averaging with the multiple sampling points, the quality of the resulting signal is

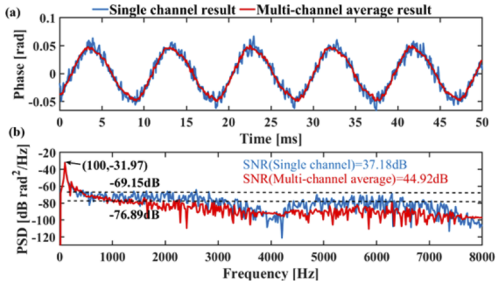

Fig. 8. Demodulation results: (a) time domain; (b) frequency domain (blue curve: single-channel result obtained with the proposed method; red curve: average multi-channel result obtained with the proposed method).

significantly enhanced. The SNR is improved to 44.92 dB, and the value of the SNR increase is 7.74 dB.

In this Letter, we have demonstrated a stable and high-SNR homodyne demodulation by using a three-step-phase-shifted double pulse based on a UWFBG array. Different from the conventional method, the introduction of the phase modulation technology and the UWFBG array ensures a more stable result and reduces the complexity of the system. Homodyne detection brings the ability to achieve fast positioning, and the UWFBG array provides multi-channel results that improve the SNR. The experimental results show that the dynamic strains can be easily positioned and accurately measured. Moreover, the SNR can be improved by 6 times by utilizing the multi-channel signals on the grating. Considering its advantages of good stability, a simple structure, a high SNR, freedom from reference light, and fast positioning, this proposed method may potentially have broad applications in complicated fiber-sensing scenarios.

Funding. National Natural Science Foundation of China (61975076, 62175100, U2001601); Qing Lan Project of Jiangsu Province; The Key Technology R&D Program of Inner Mongolia Autonomous Region (2019GG374).

Disclosures. The authors declare no conflict of interest.

Data availability. Data underlying the results presented in this paper are not publicly available at this time but may be obtained from the authors upon reasonable request.

REFERENCES

1. J. Xiong, Z. Wang, J. Jiang, B. Han, and Y. Rao, Opt. Lett. **46**, 2569 (2021).
2. Q. He, R. Liu, Z. Wang, X. Shang, T. Li, and L. Tang, Opt. Commun. **475**, 126215 (2020).
3. Z. Wang, J. Jiang, Z. Wang, J. Xiong, and Y. J. Rao, IEEE Sens. J. **20**, 12739 (2020).
4. B. Redding, M. J. Murray, A. Davis, and C. Kirkendall, Opt. Express **27**, 34952 (2019).
5. Z. N. Wang, L. Zhang, W. Song, X. Naitian, P. Fei, F. Mengqiu, W. Sun, X. Qian, J. Rao, and Y. Rao, Opt. Express **24**, 853 (2016).
6. X. Hui, S. Zheng, J. Zhou, H. Chi, X. Jin, and X. Zhang, IEEE Photonics Technol. Lett. **26**, 2403 (2014).
7. A. Masoudi, M. Belal, and T. P. Newson, Meas. Sci. Technol. **24**, 085204 (2013).
8. A. Masoudi and T. P. Newson, Opt. Lett. **42**, 290 (2017).
9. G. Fang, T. Xu, S. Feng, and F. Li, J. Lightwave Technol. **33**, 2811 (2015).
10. Y. Muanenda, S. Faralli, C. J. Oton, and F. D. Pasquale, Opt. Express **26**, 687 (2018).
11. A. E. Alekseev, B. G. Gorshkov, V. T. Potapov, M. A. Taranov, and D. E. Simikin, Appl. Opt. **61**, 231 (2022).